Journal of Statistical Physics, Vol. 97, Nos. 3/4, 1999

The Renormalization Group and Its Finite Lattice Approximations

Angelo Cacciuto,[1] Eric Gregory,[1] and Alex Travesset[1]

Received January 26, 1999; final May 27, 1999

We investigate finite lattice approximations to the Wilson renormalization group in models of unconstrained spins. We discuss first the properties of the renormalization group transformation (RGT) that control the accuracy of this type of approximation and explain different methods and techniques to practically identify them. We also discuss how to determine the anomalous dimension of the field. We apply our considerations to a linear sigma model in two dimensions in the domain of attraction of the Ising fixed point using a Bell–Wilson RGT. We are able to identify optimal RGTs which allow accurate computations of quantities such as critical exponents, fixed-point couplings and eigenvectors with modest statistics. We finally discuss the advantages and limitations of this type of approach.

KEY WORDS: Renormalization group; finite lattice; real space; Monte Carlo; anomalous dimension; unconstrained spins; scalar fields; ϕ^4.

1. INTRODUCTION

1.1. Scope and Organization of the Paper

Finite lattice approximations provide an alternative and, we think, largely unexplored approach to the Renormalization Group (RG).[(1)] The advantage of a direct RG approach lies in its generality as not only does it provide, in principle, a direct and complete calculation of the critical exponents of the model, but also further valuable information such as the fixed point Hamiltonian and the renormalized trajectory. In practical

[1] Physics Department, Syracuse University, Syracuse, New York 13244-1130; e-mail: cacciuto@epictet.npac.syr.edu, gregory@phy.syr.edu, alex@suhep.phy.syr.edu.

0022-4715/99/1100-0541$16.00/0

calculations, however, the apparent simplicity of the method is usually complicated because one needs to introduce further approximations (truncation in the operator basis, too few iterations of the RG, etc.). In addition there are errors inherent to the approach (finite size effects, statistical errors in numerical simulations, etc.). Models of unconstrained spins present, in addition, the problem of determining the resealing of the field.

These difficulties may be overcome if a detailed knowledge of the properties of the renormalization group transformation used are available. We discuss these properties in some detail and explain different criteria, some already known in the literature, to single out the best renormalization group transformation and determine the anomalous dimension of the field.

This paper is organized as follows. In Section 2 we discuss first some general aspects of the Renormalization Group (RG) and the Monte Carlo Renormalization Group (MCRG) technique. We then describe the parameterizations of the effective Hamiltonians generated along the RG flow more appropriate for the kind of approximation to be applied. We finally introduce the particular RGT to be used in this paper and we discuss the physical meaning of the parameters involved.

In Section 3 we address the problems and subtleties that appear in the finite lattice approximations of the RG. We first discuss the theoretical aspects and then explain different methods and techniques to be used in practice. We also discuss on the different sources of possible errors involved.

The technical details of the algorithms used, as well as the description of the actual parameters of the simulation, are presented in Section 4.

In Section 5 we present in detail the numerical results concerning short-rangeness of the effective interactions generated along the flow, optimization of the transformation, determination of the anomalous dimension, calculation of the critical exponents and the estimate of the different errors involved in the calculation.

The results presented in Section 5 are rather technical, so we summarize them in the first part of the conclusions. In the second part we discuss further improvements and future outlook. Some technical issues are discussed in the appendices.

2. THE RG

2.1. Some Generalities of the RG

The idea of the RG[1] is simple; average out short-distance modes leaving large distance properties intact. Let us assume that our model of

interest is described by the Hamiltonian (so called canonical surface in the RG language)

$$\mathscr{H}^0[\phi] = \sum_\alpha K_\alpha^0 O_\alpha(\phi) \tag{1}$$

where $\{K_\beta^0\}_{\beta=1,\ldots}$ are the couplings and $\{O_\alpha\}_{\alpha=1,\ldots}$ an arbitrarily chosen basis of operators. The integration of short-distance modes is implemented by a transformation $\mathscr{R}$, the Renormalization Group Transformation (RGT), whose result is to define a new effective interaction $\mathscr{H}^1$ which we parameterize with the same basis of operators as the canonical surface. The net effect of the RGT is a transformation in the space of all possible couplings of the model,

$$K_\alpha^1 = \mathscr{R}_\alpha(\{K_\beta^0\}) \tag{2}$$

Iteratively applying Eq. (2) we generate a sequence of points in coupling space that define a trajectory. We can visualize, then, the effect of a particular RGT as trajectories flowing in coupling space. Usually, these trajectories converge to a special point, say $\{K_\alpha^*\}_{\alpha=1,\ldots}$, a fixed point (FP). It is a fixed point of the RGT Eq. (2),

$$K_\alpha^* = \mathscr{R}_\alpha(\{K_\beta^*\}) \tag{3}$$

The importance of a FP speaks for itself. The universal properties of all Hamiltonians lying in trajectories converging to this FP are completely characterized by the RG flow in an infinitesimal vicinity around it;[1] all the critical exponents, for example, just follow from diagonalizing the matrix

$$T_{\alpha\beta} = \left.\frac{\partial \mathscr{R}_\alpha(K)}{\partial K_\beta}\right|_{\{K_\gamma^*\}} \tag{4}$$

In this way, the RG provides a completely general and exact prescription to compute the critical properties of any model.

2.2. The MCRG Method

The exact T matrix is a difficult object to compute. There are a number of approaches available, but as our interest lies in applying numerical techniques, we seek an expression for the T matrix as a function of expectation

values of operators. Remarkably, this can be achieved.[2] At the $(i+1)$th iteration of the RGT Eq. (2) one can easily prove[2]

$$\left.\frac{\partial \mathscr{R}_\alpha(K)}{\partial K_\beta}\right|_{\{K_\gamma^i\}} = \sum_\gamma \mathrm{H}^{-1}_{\alpha\gamma}\mathrm{M}_{\gamma\beta} \tag{5}$$

with γ running over all possible operators and

$$\begin{aligned} \mathrm{M}_{\gamma\beta} &= \langle O_\gamma^{(i+1)} O_\beta^{(i)} \rangle - \langle O_\gamma^{(i+1)} \rangle \langle O_\beta^{(i)} \rangle \\ \mathrm{H}_{\gamma\beta} &= \langle O_\gamma^{(i+1)} O_\beta^{(i+1)} \rangle - \langle O_\gamma^{(i+1)} \rangle \langle O_\beta^{(i+1)} \rangle \end{aligned} \tag{6}$$

These are expectation values of operators at the ith and $(i+1)$th iteration of the RGT, but can be computed using $\mathscr{H}^k$ with $k \leqslant i$. If $\mathscr{H}^i$ is the FP-Hamiltonian, which obviously is the case if $i = \infty$, Eq. (5) is the exact T matrix, as defined in Eq. (4).

With the very same effort, the couplings of the effective interaction $\mathscr{H}^{(i+1)}$ can also be computed.[3] The formula is[2]

$$K_\beta^{i+1} = \frac{1}{d_\beta} \sum_\alpha \mathrm{H}^{-1}_{\beta\alpha}\, d_\alpha A_\alpha \tag{7}$$

where the H matrix is defined in Eq. (6), $A_\alpha = \langle O_\alpha^{i+1} \rangle$, and d_α is the dimension of the operator O_α, to be defined precisely later.

2.3. The Effective Interactions: Organization of the Expansion

We are interested in models of unconstrained spins. The simplest case of this type of model is the linear sigma model. This is the model to which we explicitly apply all our considerations. The canonical surface is

$$\mathscr{H}^0[\phi] = \sum_n \left\{ -\kappa\phi(n) \sum_\mu \phi(n+\mu) + \phi(n)^2 + \lambda(\phi(n)^2 - 1)^2 \right\} \tag{8}$$

where n runs all over sites of the lattice, which we take as an infinite simple square lattice, and μ runs just over nearest neighbors. Spins are unconstrained, i.e., $\phi(n) \in (-\infty, \infty)$.

Under iteration of RGTs, the new effective interactions $\mathscr{H}^i$ will certainly contain more operators than those three in Eq. (8). In general, after i-RGTs we have

$$\mathscr{H}^i[\vartheta] = \sum_\alpha K_\alpha^i O_\alpha(\vartheta) \tag{9}$$

[2] This formula applies for linear sigma models. Other models require some adaptations.

with α running over all possible operators compatible with the symmetries of the model. We need an efficient organization of the operators appearing in Eq. (9).

We consider a basis of operators constructed out of monomials centered at an arbitrary site n, consisting of powers of fields at site n and products with fields in other lattice sites. A typical monomial is

$$\mathscr{M}_{k,\mathscr{K}}(n) = \sum_{\{\vec{u},\ldots,\vec{w}\}\in\mathscr{K}} \phi(n)^{2k}\,\phi(n+\vec{u})\cdots\phi(n+\vec{w}) \tag{10}$$

where $\mathscr{K}$ is the class of all vectors that starting from some representative ones may be Constructed out of the symmetries of the lattice. The full operator is constructed by summing over all lattice sites,

$$O_{k,\mathscr{K}}(\phi) = \sum_{n} \mathscr{M}_{k,\mathscr{K}}(n) \tag{11}$$

We classify all possible monomials (and therefore the operators constructed out of them), according to their type, length (l_α) and dimension (d_α);

- *The type*: we define 4 different types, shown explicitly in Table I. Type 0 are bilinear operators. Type 1 are even powers of the lattice field at point n. Type 2 and 3 include products of bilinears and even powers of the field at site n.

- *The length* l_α: This is the maximum linear separation between fields in a given monomial. An operator with length l_α can be accommodated in a lattice as small as $(2l_\alpha+1)^d$, d being the dimensionality of the system.

- *The dimension* d_α: This is the number of product fields in each monomial.

We organize operators within a certain type in increasing length and dimension. Overall, we are performing a systematic expansion with the assumption that the RG-couplings decay rapidly both with dimension and length. We elaborate more on this in considering the properties of RGTs.

There is a last remark concerning the canonical surface Eq. (8). In this paper, the model will be considered in 2 dimensions. The most general RG flow is rather complicated as there are an infinite number of inequivalent Fps. Only those that are critical, that is, those having an infinite correlation length, will be the object of our study. From the canonical surface Eq. (8), we just can reach two of them, the Gaussian FP (GFP), which is the most infrared unstable, and the Ising FP (IFP), which is the most infrared

Table I. Operators Included in the Expansion, in the Order They Are Considered with Their Associated Dimension and Length[a]

Type 0	$\vec{u}$	d_α	l_α
$\phi(\vec{n})\,\phi(\vec{n}+\vec{u})$	(1,0)	2	1
	(1,1)	2	1
	(2,0)	2	2
	(2,1)	2	2
	(2,2)	2	2
	⋮		
	(p, q)	2	p
Type 1			
$\phi(\vec{n})^{2k}$		$2k$	0
Type 2	$\vec{u}$		
$\phi(\vec{n})\,\phi(n+\vec{u})\,\phi(n)^{2k}$	(p, q)	$2k+2$	p
Type 3	$\vec{u}, \vec{w}$		
$\phi(\vec{n}+\vec{w})\,\phi(n+\vec{u})\,\phi(n)^{2k}$	$(p, q), (r, s)$	$2k+2$	

[a] The vectors $\vec{u}=(p, q)$ are the representative vectors of the class $\mathscr{K}$ in Eq. (10). The parameter k starts at 1.

stable. To reach any other critical FP, higher operators, together with a fine tuning of the couplings, should be considered.

2.4. The Bell–Wilson RGT

There are (infinitely) many different RGTs giving rise to different RGTs having different properties. The utility of those properties lies in that they may be used to single out some RGTs as being more accurate than others in approximate calculations of the T matrix. The choice of a particular RGT is therefore determined by the type of approximation we apply.

As we are eventually interested in a finite lattice approximation, a very important property is to identify RGTs generating very short-ranged effective Hamiltonians. That is, at each RG iteration, the effective interaction $\mathscr{H}^i$ generated can be parametrized with a few operators of small dimensions and lengths. This is the case if FP couplings, for example, decrease at least as rapidly as

$$|K_\alpha^*| \lesssim e^{-d_\alpha/\xi_d} e^{-l_\alpha/\xi_l} \tag{12}$$

i.e., exponentially with both dimension and length. We introduced two decay correlation lengths ξ_l and ξ_d. The importance of this property lies in that the more short-ranged the FP, the more insensitive it will be to truncation of higher dimension and length operators. This is the rationale behind the organization of the expansion of the operators generated along the RG flow in the previous section.

The RGT first introduced in ref. 4 has the property that the Gaussian FP is short-ranged, in the sense of Eq. (12).[4, 5, 6] It is therefore a natural candidate to investigate for other Fps as well. The RGT is

$$e^{-\mathscr{H}^{i+1}[\vartheta]} = \int \prod_n d\phi(n)\, e^{-\mathscr{H}^i[\phi]} e^{-(a_W/2)\sum_{n_B}(\vartheta(n_B) - b\sum_{n\in n_B}\phi(n))^2} \tag{13}$$

where the average is over $c \times c$ cells in the fine lattice, with $c = 2$ as shown in Fig. 1. There are two a priori free parameters, a_W and b.

The parameter a_W just labels different transformations. Universal quantities are independent of it. Of course, within an approximation that may not be the case exactly, and it provides us with a freedom that we can use to optimize the performance of the RGT.

The parameter b, however, has a much deeper meaning related to the unboundedness of the spins; we may rescale them, and yet the physics of the model is the same. If there is a FP we may generate a whole line of new FPs by rescaling the field ϕ. The model shows a redundant direction.[1, 10] By definition, any point in that line is a FP of the transformation, so the RGT cannot make the FP flow along this direction, and therefore it is exactly marginal. A first consequence of this is that the T matrix will always have at least ones eigenvalue exactly equal to one. The parameter b gets uniquely and self-consistently fixed by requiring that there is no flow

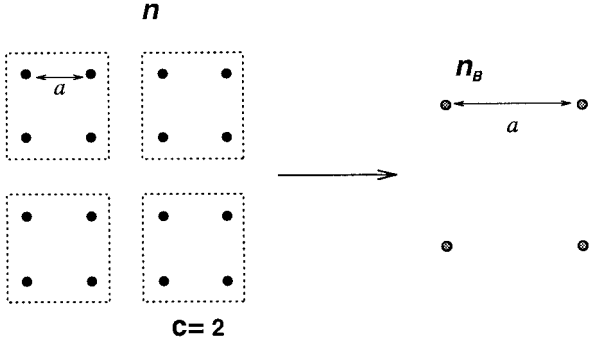

Fig. 1. Graphical representation of the short-distance integration of the RGT Eq. (13), n labels sites in the finite lattice, n_B in the coarse one.

along this marginal redundant direction. Any other choice of b would cause this line to be relevant or irrelevant, and there would be no FP in the theory, in contradiction with the physics of the model. The resealing parameter is not a freedom of the model. In fact, it has a universal meaning. It may be related to the anomalous nonformal dimension of the field η, the exponent controlling the universal algebraic decay as a function of distance of the two-point correlation function

$$G(x) \equiv \langle \phi(x)\, \phi(0) \rangle \sim \frac{1}{|x|^{d-2+\eta}} \quad |x| \to \infty \tag{14}$$

with

$$\eta = d + 2 - 2\frac{\ln b^*}{\ln c} \tag{15}$$

where b^* stands for the resealing factor b at the FP and c will be usually equal to 2.[1]

3. THE RG IN A FINITE LATTICE

3.1. Theoretical Issues

We consider now the canonical surface Eq. (8) and the transformation Eq. (13) defined on a finite lattice with periodic boundary conditions (so that translation symmetry is preserved). The T-matrix may be computed from Eq. (5) and Eq. (6). The question is how much the T-matrix computed within this approximation differs from its infinite volume value.

Let us assume that the FP of the RGT is such that the largest operator length is no. The entire FP may be accommodated in a lattice as small as $(2n_s+1)^d$. Let us consider it now in a $(2(2n_s+1))^d$ volume, and apply a RGT, reducing the volume to a $(2n_s+1)^d$. As the FP still perfectly fits in, the FP couplings should not differ from their infinite volume values. There are no finite size effects.[3] This is even more remarkable when one considers that both the couplings and the T-matrix are computed from the matrices Eq. (6). These involve the computation of expectation values that show severe finite size effects as the system is critical, and hence has infinite correlation length. This may be one of the most interesting features of MCRG methods. We may, at least in principle, obtain infinite volume results working within a finite lattice approximation. Finite size effects are

[3] More rigorously, finite size effects are exponentially suppressed and therefore very small. They are irrelevant for this argument.

not dictated by the correlation length (which is infinite) but by the range of the FP (and therefore of the RGT). A consequence of the previous arguments is that the parameters of the canonical surface must be fine tuned at criticality. We need to perform the calculations at the values of the exact critical surface of the infinite dimensional system, at virtually infinite correlation length.

Obviously, applying a RGT in a finite lattice reduces its volume. Even if the RGT is very short-ranged, it may happen that the FP cannot be reached before the lattice is so small that huge finite-size effects, as explained, enter into the game. As we may iterate the RGT only a finite number of times, we need RGTs such that the canonical surface is very close to the FP.[7, 8]

In short, any RGT to be used in a finite lattice approximation should fullfill two conditions;

- *Generate short-ranged effective Hamiltonians.*
- *Approach the FP rapidly.*

In models of unbounded spins there is still the issue of the determination of the rescaling factor b in the RGT Eq. (13). This parameter is intimately related to the existence of a line of FPs. In general, however, not all FPs along this line will be short-ranged enough and the existence of the whole line may be apparent only in going to prohibitively large lattices. However, if a sufficiently short-ranged FP exists, we may expect at least an infinitesimal portion of this line to survive around it and the T matrix to exhibit at least one eigenvalue equal to one with good precision.

3.2. RG in Practice

The critical couplings of the canonical surface Eq. (8) in an infinite lattice cannot be computed within a MCRG approach. It is a quantity to be computed from other techniques, and we extracted it from the analysis of existing coefficients of the strong coupling expansion of the canonical surface, as discussed in Appendix A.

Once the critical couplings are known, iteration of the RGT Eq. (13) would drive the canonical surface towards the most infrared stable FP, the Ising FP (IFP) our model. The strategy we follow is to pick a value for a_W (see Eq. (13)) and apply as many RGTs as allowed (that is, until the lattice becomes a 4^2 volume) with different values for the resealing value b (as defined in Eq. (13)). In the previous subsection we discussed the different issues that need to be addressed. The different criteria we used to tackle them are as follows,

1. *Short-ranged effective Hamiltonians*:

(a) Using Schwinger–Dyson Eq. (7) we compute the couplings and check for the ansatz Eq. (12).

2. *Rapid approach to the FP*: There are two different criteria to be met.

(a) If a FP is reached, the couplings of these effective Hamiltonians after successive applications of RGTs should coincide.

(b) we perform RGTs starting from the same canonical surface but in a smaller lattice and compare expectation values of operators at the same volume size. If a FP is reached these expectation values should agree.

3. *The determination of the anomalous dimension* η

(a) The T matrix should exhibit an exactly marginal eigenvalue at the right value of the resealing factor.

(b) Similarly as in criterion 2(b), the expectation values of operators should agree at the correct value of the anomalous dimension.

We then scan over different values of a_W and select the values optimally fulfilling all previous criteria.

Criteria 1(a) and 2(a) are obvious. Criteria 2(b) uses the fact that although finite size effects for these expectation values are huge, they enter in exactly the same functional form,[9] and if a FP is reached, those expectation values should agree. Criterion 3(a) to pick up the anomalous dimension is a modification of.[4] It was first introduced in[11] and successfully applied to the linear sigma model in 3 dimensions, although the lattices used were slightly too small, and finite size effect errors were difficult to assess. Criterion 3(b) is a necessary consequence of the discussion in criterion 2(b) and the fact that a wrong choice for b should not lead to a FP at all.

Besides the statistical errors inherent in any numerical simulation, there are different sources of putative systematic errors,

- $e(1)$ *Truncation errors*: If some operator having a sizeable coupling is not included in Eq. (5) and Eq. (7) the H and M matrices miss sizeable matrix elements which translates into systematic errors in the determination of both the T matrix and the couplings.
- $e(2)$ *Finite size effects*: This error appears when the lattice is too small to accommodate operators having sizeable couplings.
- $e(3)$ *Off-criticality*: If the couplings in the starting Hamiltonian are not tuned to criticality, the flow eventually converges towards the renormalized trajectory, moving away from the FP.

• $e(4)$ *Lack of eigenvector convergence*: It may happen that some eigenvectors of the T matrix are just not convergent, in the sense that the coefficients defining it have just a formal meaning. This may translate into the corresponding eigenvalue being completely unreliable.

• $e(5)$ *Redundant operators*: Some eigenvalues may depend on the transformation, the associated critical exponent is then just an artifact of the transformation.[12, 13]

Finally, let us recall that in models of unconstrained spins, like the ones we are interested in, the resealing itself will have an associated error bar due to statistical errors and e(1), e(2) and most importantly e(3). This rescaling error bar the will translate into an additional error in computing other quantities.

4. NUMERICAL DETAILS

4.1. The Algorithm

We use an embedding algorithm,[14] each step consisting of 15 cluster-Wolff updates[15] and 5 metropolis hits. We need 20 sweeps of this type to completely decorrelate data. We computed the error as a function of bin-size using standard Jackknife techniques and found a flat plateau showing that data in different bins are totally uncorrelated. After thermalization, we generated 64,000 decorrelated 64^2 lattice configurations and 50,000 34^2 lattice configurations at criticality, and stored them in disk. The uncompressed storage size of these is about 2 GB and 500 MB respectively. The simulation was carried out on a 233 MHz Pentium processor, and took about 2 days of total CPU time.

In order to compute the H and M matrices in Eq. (6), one must perform a full Monte Carlo simulation of Eq. (13) which becomes slightly complicated because it depends on two variables, ϕ and ϑ. Fortunately, as it is apparent from Eq. (13), the ϑ variables are independently Gaussian distributed about $b\sum\phi$ in each cell for a "frozen" ϕ configuration. This allows us to implement the ϑ integration using the shift

$$\vartheta(n_B) = b \sum_{n \in n_B} \phi(n) + \frac{\zeta}{\sqrt{a_W}} \tag{16}$$

where ζ is a randomly distributed Gaussian variable with zero mean and variance 1. This trick amounts to a direct computation of the observables involving the ϑ variables first, so that H and M matrices effectively become just a function of the ϕ variables. As a final remark let us mention that we

have cross checked this procedure against a full Monte Carlo simulation and against exact analytical calculations for the Gaussian fixed point (see Appendix B).

From Eq. (16) we generate the successive RGTs. On a 233 MHz Pentium processor it takes about 100 minutes of CPU time to generate the M matrices and H matrices including up to 40 operators for 32^2, 16^2, 8^2 and 4^2 volumes.

4.2. The Method

The canonical surface Eq. (8) is a actually a line $\kappa(\lambda)$. We performed our simulations at $\lambda = 1.0$, with corresponding $\kappa(1.0) = 0.6795$.

Concerning the expansion of the effective Hamiltonians generated along the RG flow, we considered up to 40 operators in total. All operators of type 0 up to length 3, operators of type 1 up to dimension 10, operators of type 2 up to length 3 and dimension 6, and operators of type 3 up to length 2 and dimension 4, as defined in Table I. In the discussion that follows we will identify these operators by number from 1 to 40. Operators 1 to 5 correspond to type 1 $k = 1,...5$. Operators 6 to 14 correspond to type 0 operators $(p, q) = (1, 0),..., (3, 3)$. Operators 15 to 23 correspond to type 2 operators with $k = 1$ $(p, q) = (1, 0),..., (3, 3)$. Operators 24 to 32 correspond to type 2 operators with $k = 2$ $(p, q) = (1, 0),..., (3, 3)$. Operators 33 to 40 are the eight distinct $k = 1$ type 3 operators that fit in a 3×3 section of lattice ($\vec{n}$ at the center): $[(p, q)(r, s)] = [(0, 1)(0, 1)]$, $[(0, 1)(1, 0)]$, $[(0, 1)(0, -1)]$, $[(0, 1)(1, 1)]$, $[(0, -1)(1, 1)]$, $[(1, 1)(-1, 1)]$, and $[(1, 1)(-1, -1)]$.

We systematically explored anomalous dimensions $\eta = 0.10$, 0.20, 0.25, 0.30, 0.40, 0.50. In some particular cases additional values were also considered. To improve the performance of the transformation, we studied the following values of the RGT parameter: $a_W = 8,16, 20, 40, 80, \infty$.

In order to efficiently handle the enormous amount of data generated, we organized the information in different *html*-tables, each one displaying the particular property under study. Samples of tables are available at the address http://web.syr.edu/~acacciut.

5. RESULTS

In this section we present an extensive and detailed analysis of the methods and techniques already introduced. We keep the discussion technical. The main results may appear a little dispersed, so in the next section we provide a presentation of the most relevant final results and the different implications they may have.

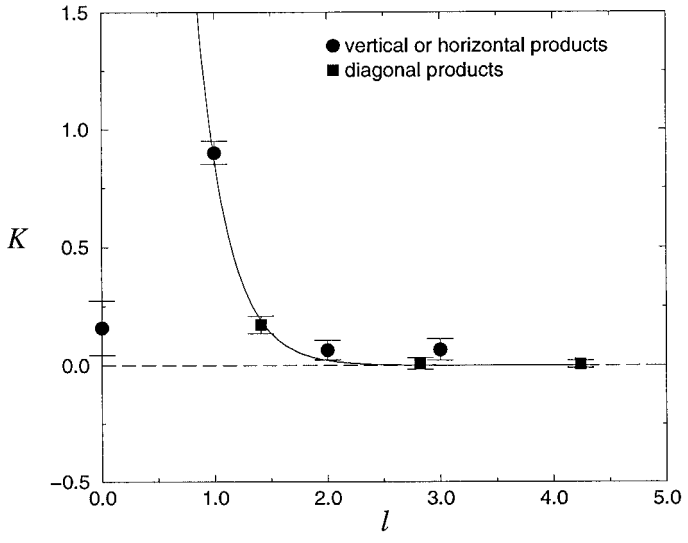

Fig. 2. Plot for $a_W = 16$, $\eta = 0.30$ of the magnitude of type 0 (bilinear) couplings as a function of length for 3 RGTs. Squares are vertical or horizontal products and circles the diagonal ones. The solid line is an exponential decay.

5.1. Short-Ranged Hamiltonians

The effective interactions generated along the RG flow depend on a_W (the transformation) and b (the rescaling). The subject under study now is the decay of couplings with dimension and length as a function of a_W for a given b. The optimal RGT will be the one generating the most short-ranged effective interaction.

The first issue to address is the dependence of couplings on length. All the different values of a_W examined conform to the decay ansatz Eq. (12), although the decay is too fast to allow a precise determination of the correlation length decay ξ_l, as coupling constants are zero within statistical error bars for $l \geqslant 2$. The typical situation occurring for any value of a_W is plotted in Fig. 2.[4] From the data in Fig. 2 we can give a very conservative upper bound for the correlation length decay,

$$\xi_l < \tfrac{1}{2} \tag{17}$$

valid for any value of a_W. We conclude that operators have a very good decay property for any a_W value as far as length is concerned.

[4] We generalize slightly the definition of length by giving length $\sqrt{2}$ to the operator (1,1) instead of 1, as defined.

Couplings as a function of dimension show a very strong dependence on a_W. In Fig. 3 a logarithmic plot of the magnitude of type 1 couplings is shown as a function of dimension. For small a_W the decay ansatz, Eq. (12), sets in for small values of dimension. For $a_W = 8$, we extract a dimension correlation length decay

$$\xi_d \sim 1.0 \tag{18}$$

The correlation length decay as a function of distance is slower than with length. Increasing a_W further, there is a transient increase of couplings, with a peak moving forward in dimension as a function of a_W, before the asymptotic form Eq. (12) becomes apparent, as shown in Fig. 3. In particular, the RGT at $a_W = \infty$ shows a remarkably poor behavior.

We cross-check previous results by studying the decay of type 2 operators. As shown in Fig. 4, couplings decay exponentially, with a correlation length completely compatible with the bound in Eq. (17).

From all the evidence accumulated, it is clear that smaller values a_W restrict the dependency of the effective interactions to lower dimension field operators. In particular, effective interactions generated with RG transformation with $a_W \geqslant 80$ are not particularly recommended, as the couplings decay too slowly with dimension to obtain reliable results.

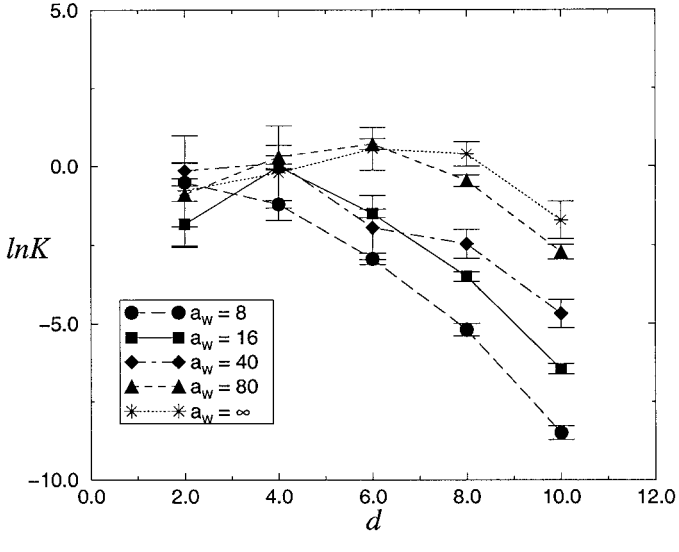

Fig. 3. The logarithmic plot of the magnitude of type 1 couplings against dimension, d. Results are for 3rd RGT at $\eta = 0.30$.

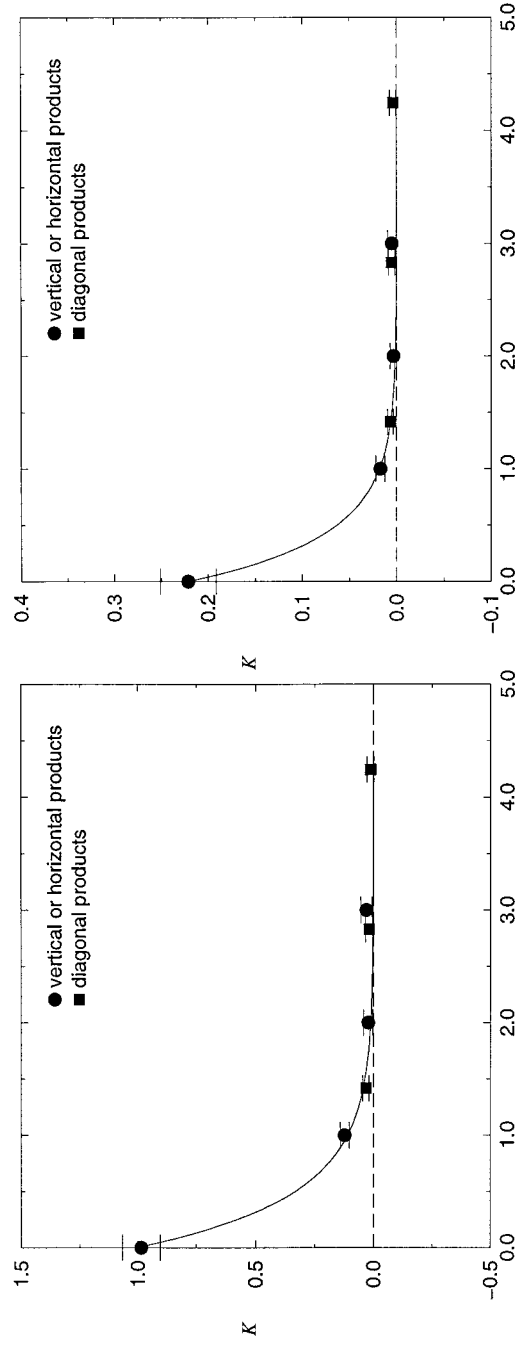

Fig. 4. Decay of type 2 couplings against length for $k = 1$ (left) and $k = 2$ (right) (see Table I for definitions) operators against length. Results are for 3 RGTs at $a_W = 16$, $\eta = 0.30$. The solid line is the exponential fit, which is in agreement with Eq. (17).

Table II. Example of Couplings at 2(up) and 3 RGTs(down) for $a_W = 40$ That Match Poorly

η	1	9	11	18
0.25	−0.6(2)	0.02(5)	−0.03(7)	0.002(20)
	−1.1(3)	0.19(4)	0.15(8)	−0.08(3)
0.30	−0.40(20)	−0.03(7)	−0.03(7)	−0.005(20)
	−0.87(21)	0.12(4)	0.14(8)	−0.09(2)
0.40	−0.40(20)	0.03(5)	−0.03(6)	−0.003(20)
	−0.56(24)	0.17(3)	0.12(7)	−0.06(2)

5.2. Fast Approach to the FP

The effective interactions show a double dependence on the rescaling b and on the parameter a_W. The dependence on b is related to the determination of the anomalous dimension and will therefore be studied in the next subsection. Now we content ourselves with identifying the RGTs that converge rapidly to putative FPs.

Concerning criterion 2(a), the matching between couplings in successive RGTs, although the amount of information that may be extracted is certainly limited by the somewhat large statistical errors in the couplings, it is still powerful enough to provide strong evidence that we approached a FP after a few RGTs. For values of $a_W \geqslant 80$ couplings from successive RGTs do not match satisfactorily, and we cannot identify a FP for any value of the resealing. In agreement with previous results, RGTs with large a_W values perform very poorly. We move on to investigate lower values for a_W. Results at $a_W = 40$ do not show a clear FP for any value of the rescaling, as there are some couplings that do not agree within 2σ (statistical), see Table II.

For $a_W = 8$, there is no clear evidence for a FP at $\eta \geqslant 0.30$, see Table III, although we find an acceptable matching for smaller values of η.

Table III. Example of Couplings at 2(up) and 3 RGTs(down) for $a_W = 8$ with Rather Poor Matching

η	1	18	21	30
0.30	0.67(7)	0.014(6)	0.001(5)	0.0001(5)
	0.60(6)	0.00(1)	0.015(6)	−0.0020(7)
0.40	0.52(6)	0.012(5)	−0.001(4)	−0.0000(4)
	0.38(6)	−0.003(4)	0.012(4)	−0.0015(6)
0.50	0.39(6)	0.010(4)	0.001(4)	−0.0000(4)
	0.19(6)	−0.003(3)	0.010(4)	−0.0010(4)

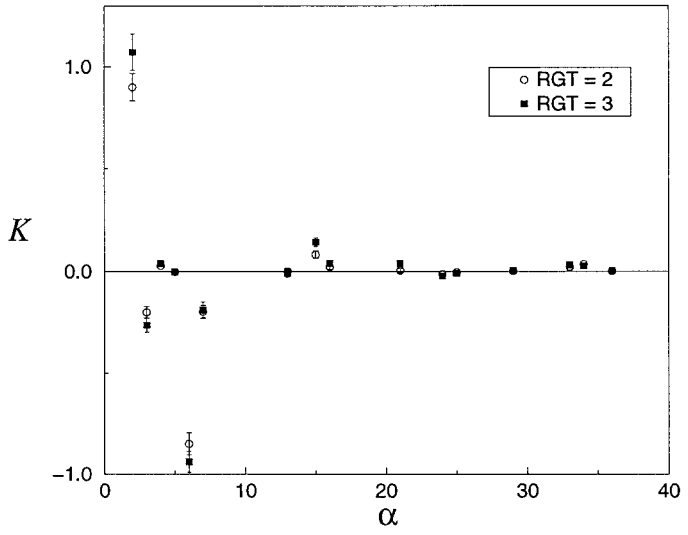

Fig. 5. Some chosen couplings at $a_W = 16$ and $\eta = 0.25$ for 2 and 3 RGTs.

The value of $a_W = 16$ shows putative FPs within the statistical errors for values of the anomalous dimension in the range $\eta = 0.20 - 0.40$. As an example, in Fig. 5 couplings from 2 and 3 RGTs are plotted at $\eta = 0.25$. It is apparent that most of the couplings agree very well. It seems then that $a_W = 16$ is an optimal choice according to criterion 2(a).

Concerning criterion 2(b), the matching of expectation values of operators computed using different lattice sizes, we start by defining the quantities

$$r_\alpha^{(i)} = \left| \frac{\langle O_\alpha^{(i)} \rangle - \langle O_\alpha^{(i-1)} \rangle}{\langle O_\alpha^i \rangle} \right|$$
$$Q^{(i)} = \sum_\alpha (r_\alpha^i)^2 \tag{19}$$

which measure the quality of the matching for expectation values of operators. A first insight is gained from the plot of the factor $Q^{(i)}$, (see Fig. 6). There is a clear minimum independent of a_W for $\eta \sim 0.3$. This matching procedure appears to be a very precise criterion to fix the rescaling, but this a question to be considered later. What is more surprising from Fig. 6 is the very good matching of observables for any value of a_W including values for which we do not find evidence for a FP from

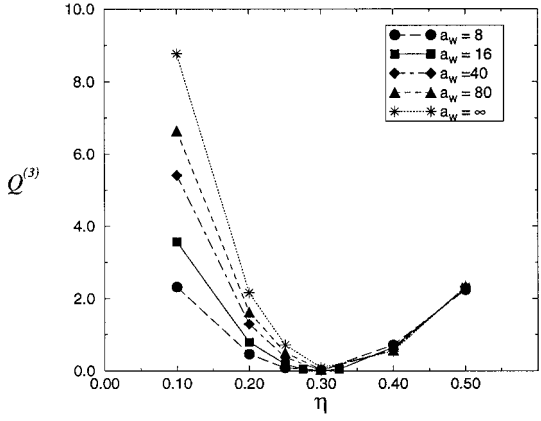

Fig. 6. Dispersion in the matching of expectation values of operators, comparing 3 RGTs starting at 642 with 2 RGTs starting at 32^2.

criterion 2(a). However, criterion 2(b) is completely insensitive to the truncation of operators and to finite size effects, the systematic errors that affect criterion 2(a) the most, but is very sensitive to the canonical surface not being critical, which probably accounts for the small systematic error in η (the exact value is $\eta = 0.25$). A closer inspection, reveals that the quality of

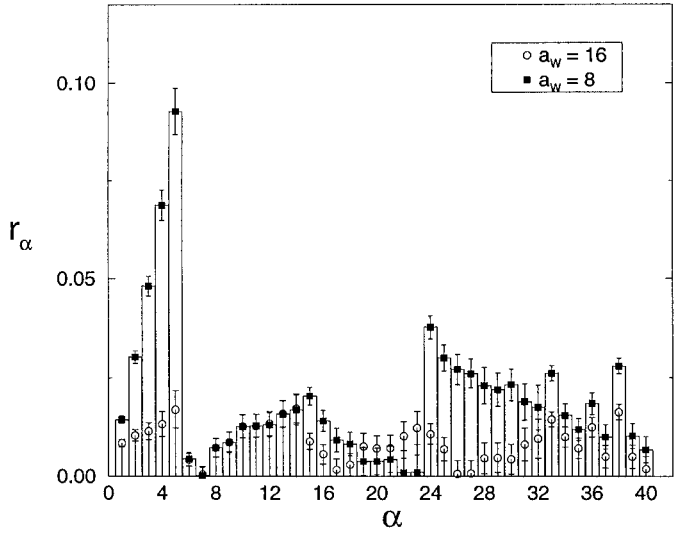

Fig. 7. Comparison of the quantity r_α, as defined in Eq. (19) for $a_W = 8$ and $a_W = 16$ as computes from 3 RGTs starting at 64^2 and 2 RGTs starting at 32^2. The RGT with $a_W = 16$ produces a better matching.

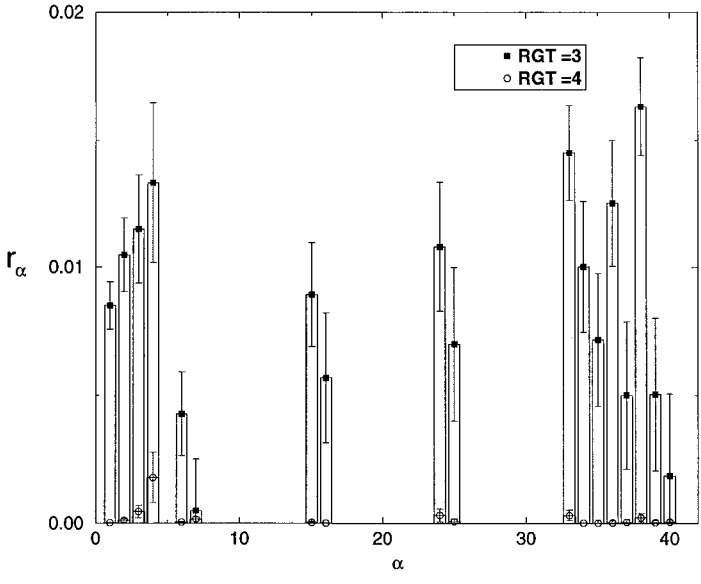

Fig. 8. Comparison of r_α after 4/3 (4^2 lattice) and 3/2 RGT (8^2) lattice at $\eta = 0.30$. Only operators that can be accommodated in a 4^2 lattice are plotted. The matching is nearly perfect.

the matching is sensitive to a_W. As apparent from Fig. 7, a careful comparison shows that the approach to the FP is faster for a transformation at $a_W = 16$.

To cross-check criterion 2(b) further, we compared the matching of observables on the next RGT, that is, observables computed in a 4^2 lattice. The number of operators available gets reduced, as some of them can no longer be accommodated in such small lattice, but for those that it exists, the matching should significantly improve as compared with the previous RGT. This is, indeed, corroborated from Fig. 8, the matching in this case is close to perfect.

5.3. The Determination of the Anomalous Dimension

Previous considerations have selected the value of $a_W = 16$ as the one best compromising the 2 criterion of short-rangeness and fast approach to the FP. We now come to the determination of the rescaling factor, which as a byproduct allows us to compute the first critical exponent of the theory, the conformal anomalous dimension, see Eq. (15). We devised two different criterion to be meet.

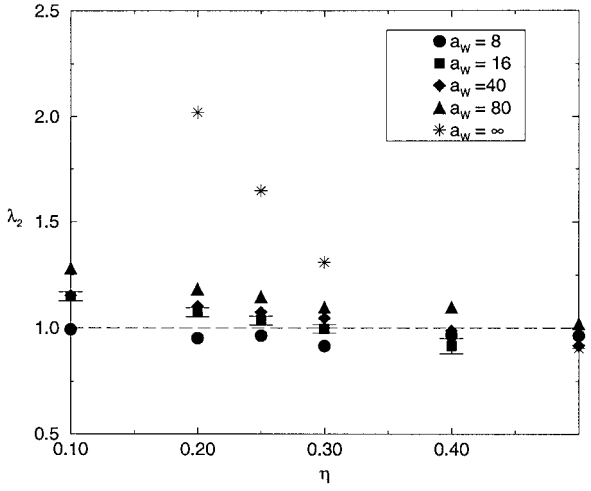

Fig. 9. The second eigenvalue of the T matrix as a function of the anomalous dimensions for different values of a_W after 2 RGTs.

The first criterion 3(a) is the proper identification of a marginal eigenvalue in the T matrix. In our particular problem, this is complicated by the fact that in the cases were the two criteria we use to determine that a FP is reached, we clearly get two marginal directions. It seems natural to assume generally that the model has actually two marginal directions. Although we already ruled out some values of a_W, we keep the discussion general for the time being and consider all values. The second eigenvalue of the T matrix as a function of η is plotted in Fig. 9 for 2 RGTs. Large values of a_W are incompatible with the T matrix having a marginal eigenvalue, except for large values of the anomalous dimension, where the third eigenvalue is far from one, and following previous discussions should be disregarded. This is reassuring, since for those values of a_W we already know that RGT perform rather poorly. For smaller values of a_W, we do get a one eigenvalue within statistical error bars in the range $0.10 < \eta < 0.40$. If a FP is reached, the marginal eigenvalue should be stable through the next RGTs, plotted in Fig. 10. Also, for small values of η, which criterion 3(b) will rule out as well, the third eigenvalue is clearly different from one. Within statistical error bars, the window of anomalous dimensions is further restricted to be in the range $0.25 \leqslant \eta \leqslant 0.30$.

The matching between operators, criterion 3(b) turns out to be the most sensitive criterion, a result already anticipated in Fig. 6. For our favorite value $a_W = 16$, all expectation values of operators match for

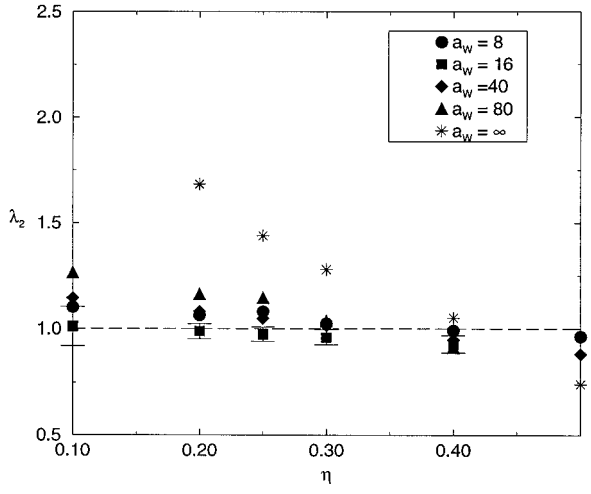

Fig. 10. The second eigenvalue of the T matrix as a function of the anomalous dimensions for different values of aw after 3 RGTs.

$\eta = 0.30$ within 2σ in the statistical error bars, for all 40 operators considered, see Fig. 11. For comparison, we plot as well the relative error for values of the anomalous dimensions $\eta = 0.10$ and $\eta = 0.50$ in which there is no matching at all. Let us recall that if we perform another RGT, the matching is perfect see previous Fig. 8. This provides an important cross-check that we are in the vicinity of the IFP. Unfortunately, the final lattice (4^2) is too small and shows finite size effects in the critical exponents, as we will discuss.

The matching criterion singles $\eta \sim 0.30$ as the preferred value for the anomalous dimension, a result slightly off from the exact value, $\eta = 0.25$. The matching at $\eta = 0.25$ is also good but not as good as in $\eta = 0.30$. We will expand further on this issue in the discussion of the different sources of systematic errors.

5.4. The critical Exponents and the FP Hamiltonian

The rescaling parameter has been computed and it corresponds to an anomalous dimension in the interval at $\eta \in (0.25, 0.30)$, our results favoring values closer to $\eta = 0.30$ than to $\eta = 0.25$.

In Fig. 12 we plot the first eigenvalue as a function of the rescaling parameter. The first eigenvalue is very sensitive to the value of the anomalous dimension. Statistical errors are relatively small, certainly very

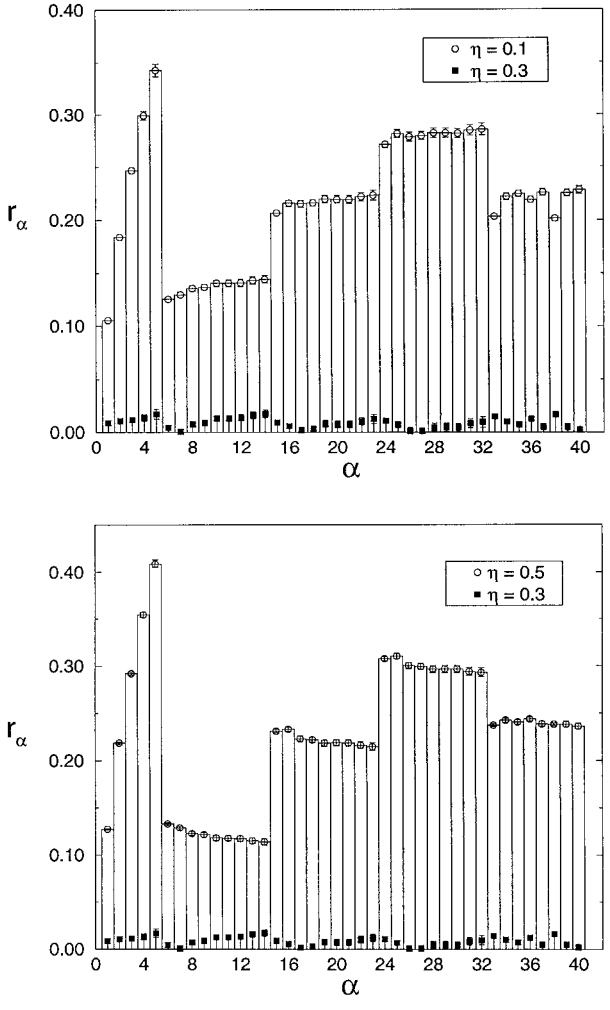

Fig. 11. Plot of the quantity r_α as defined in Eq. (19) comparing the excellent matching at $\eta = 0.30$ with no matching at all at $\eta = 0.10$ (top) and $\eta = 0.50$ (bottom). The final lattice is 8^2.

small when compared with the error bars in the couplings. The first eigenvalue for the interval of anomalous dimensions considered is

$$\begin{aligned} \eta &= 0.25, \qquad \lambda_1 = 2.015(7) \\ \eta &= 0.275, \qquad \lambda_1 = 1.996(7) \\ \eta &= 0.30, \qquad \lambda_1 = 1.976(7) \end{aligned} \tag{20}$$

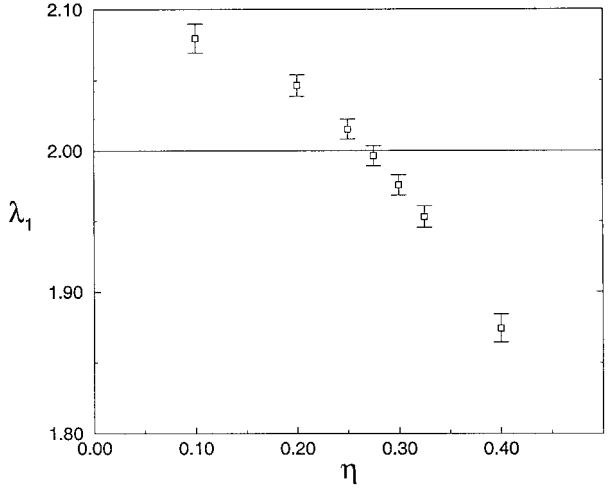

Fig. 12. First eigenvalue as a function of the anomalous dimension at $a_W = 16$, final lattice is 8^2.

where the error is just statistical. Results are obtained after 3 RGTs, in a 8^2 lattice, so that finite size effect errors are smaller than the statistical ones, as will be discussed.

In Fig. 13 the third eigenvalue is plotted and as already pointed out, it is compatible with one.

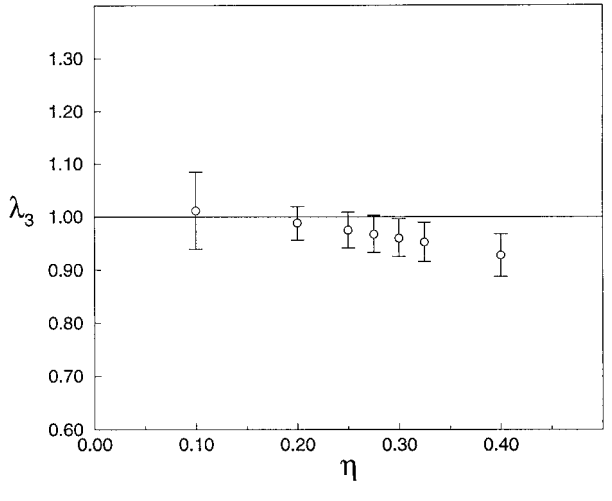

Fig. 13. Third eigenvalue as a function of the anomalous dimension at $a_W = 16$, final lattice is 8^2.

We can compute the FP action. For consistency with our analysis, we will quote the results at $\eta = 0.30$, although given the relative large error bars, it is essentially insensitive to η within the range (0.25, 0.30).

5.5. The Different Sources of Errors

We now analyze the different sources of errors that may appear. We treat each case separately.

5.5.1. Error e(1). This is the systematic error that may appear if some operators having sizeable coupling are not considered into Eq. (6). From previous results, we obtained that FP couplings decay at least exponentially, both with length and distance, and, as we parametrized the effective interactions generated along the flow within this assumption, we should not expect large systematic errors coming from truncation effects.

In the case of the evaluation of couplings, a typical plot of the evolution in the value of the coupling as more operators are considered is shown in Fig. 14. Results are strongly sensitive to the inclusion of higher dimension operators but rather mildly to length. Furthermore, statistical error bars grow considerably with the inclusion of more operators. Eventually there is flat plateau, but only after enough number of operators are included. If we assume that the systematic error coming from the truncation, consistently with previous assumptions, decays exponentially, we estimate that is smaller than the statistical error. Although the truncation

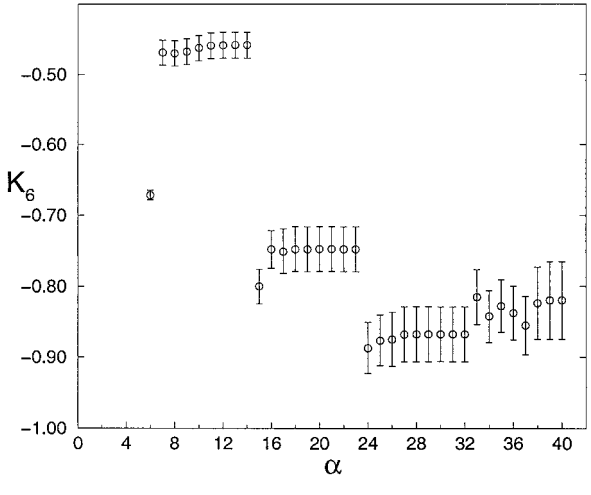

Fig. 14. Evolution of coupling 6 as a function of operators included.

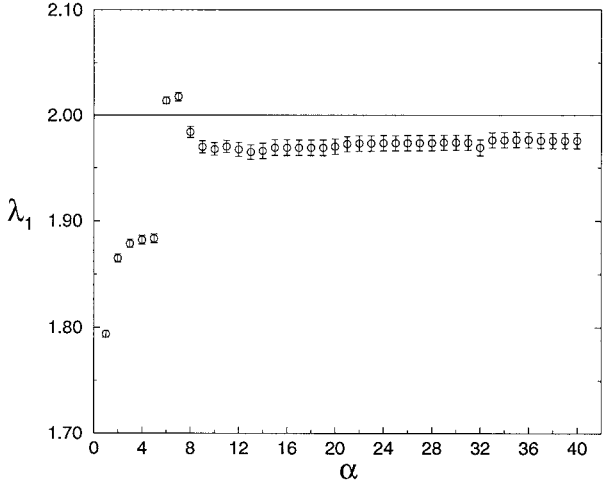

Fig. 15. Evolution of the first eigenvalue as a function of operators included.

error is not completely negligible, statistical errors should be diminished to make it apparent. In other words, if larger statistics were available, higher dimensional operators should be considered.

Concerning the evolution of eigenvalues, we do find a flat plateau which sets in with the inclusion of relatively few operators, see Fig. 15 and Fig. 16. For the case of eigenvalues we cannot find any evidence for a significant systematic error coming from the truncation.

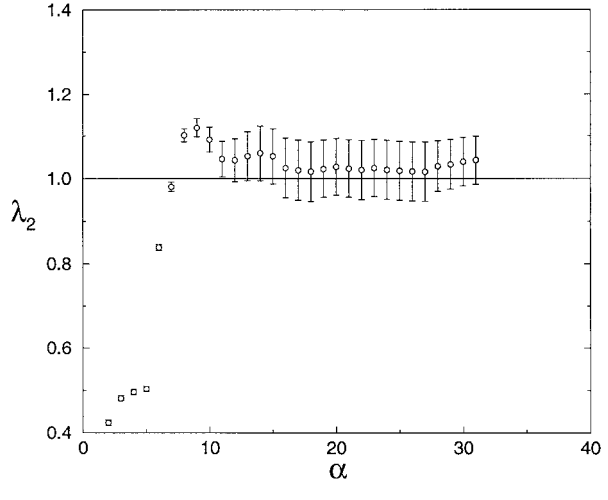

Fig. 16. Evolution of the second eigenvalue as a function of operators included.

We conclude that the operators induced are consistent within the statistics we considered. Errors coming from the truncation are smaller than the statistical one.

5.5.2. Error e(2). Finite size effects enter into the game when there are operators with sizeable coupling constants whose length is greater than the linear size of the lattice, L. Both the couplings and eigenvalues will then acquire a dependence on L. Of course this error should be more apparent as the lattice is smaller. Our results at a 4^2 do show finite size effects, but as our main conclusions are drawn from the analysis of a 8^2 lattice, we analyzed the effect in those. In Fig. 17 we compare the couplings of the effective interaction generated after 2 RGTs starting from a 32^2 and 64^2 lattices respectively. If there are finite size effects, these couplings should differ as they have different L dependences, irrespective of how we truncated the expansion (we truncate it in the same way in both lattices), and if we are reaching a FP (this is a question addressed by comparing successive RGTs). From Fig. 17 we cannot detect a significant dependence on L within statistical errors. We conclude then, that finite size errors are within statistical ones if the smallest lattice used is a 8^2 one.

5.5.3. Error e(3). If the canonical surface is not exactly at criticality, the right infrared FP cannot be reached. The RG trajectories eventually flow towards the renormalized trajectory instead, and the matching

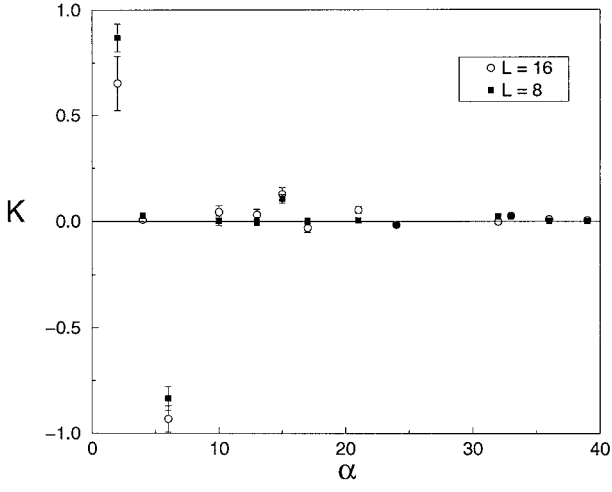

Fig. 17. Comparison of couplings at $a_W = 16$, $\eta = 0.275$ computed after 2 RGTs starting from a 64^2 and 32^2 lattice respectively.

procedure should eventually deteriorate. Unfortunately, we cannot perform more RGTs to check if this is the case, and we do not have a more precise estimate of the critical couplings to compare with the results already obtained. From the matching criterion (precisely the method more sensitive to this error) $\eta = 0.30$ is clearly preferred and the matching criterion is just marginally consistent with the exact result $\eta = 0.25$. This makes us suspect that there is a small systematic error of this kind in our calculations, which unfortunately we cannot estimate.

5.5.4. Error e(4). This error is associated with the transformation, and it is not peculiar to a finite lattice approximation. It appears when couplings in eigenvectors fail to converge.

For the sake of clarity, in the appendix Section B we present a simple model that can be solved exactly (the Gaussian model), where an explicit example of this problem is shown.

An obvious criterion to detect this problem seems to compute the eigenvectors, diagonalizing the T matrix, explicitly checking that they decrease as a function of length and dimension. For the first three eigenvalues (the 2 and the two 1s) that we already computed we do not find a decay of the eigenvector components as apparent as it was with the FP couplings. The next two eigenvalues at $a_W = 16$ and $\eta \in (0.25, 0.30)$ form a complex pair, so we think that those eigenvalues are affected by error e(4). As the eigenvectors are complex as well, we do not know how to extract any consequence from the analysis of the coefficients. In any case, let us mention that finite lattice approximations to simpler models do also show complex pairs when the eigenvectors fail to converge, so it may be the case here as well. More statistics should clarify this issue.

6. CONCLUSIONS

6.1. Summary of the Results

Un this paper we studied finite lattice approximations in models of unconstrained spins. We discussed the properties that a renormalization group transformation should have in order that a finite lattice approximation may be organized into a controlled and systematic expansion, able to give accurate and rigorous results; we also discussed the difficulties that appear in computing the anomalous dimension of the field.

As a non-trivial example, we studied the linear sigma model in two dimensions in the domain of attraction of the Ising fixed point, using the Bell–Wilson RGT,[4] which has a free parameter a_W. The properties of the RGT depend on aw and the goal was to properly identify the values of

a_W that optimally fullfill the two important properties relevant for us, the short-rangeness of the effective interactions generated and a rapid approach to the Ising fixed point.

To address the issue of how short-ranged are the effective interactions essential use has been made of the Schwinger–Dyson equations Eq. (7) criterion 1(a). Overall the method performs well, but the statistical error bars are relatively large, which in some cases limits the accuracy of the results. In any case, we have provided convincing evidence that the decay ansatz Eq. (12) is well satisfied (see Figs. 2–4), which in turn provides the justification for the expansion we propose for the effective interactions. Our results clearly show that the smaller the value of a_W the better the decay properties and that decay with dimension is slower than with distance. If more statistics would be available, the expansion should include more higher dimensional operators than higher length.

Although the smaller a_W, the more short-ranged the fixed point action is, we found that for slightly higher values ($a_W \sim 16$) the canonical surface is closer to the corresponding FP. To reach this conclusion we computed the couplings generated after successive RGTs and checked whether they agree, criterion 2(a). This was helpful to rule out high values of a_W, and to provide strong evidence for a FP at $a_W = 16$ ($\eta = 0.25$) (see Fig. 5). We also used the matching criterion of observables 2(b) and found only a tiny dependence on awl enough to show that $a_W = 16$ is the optimal case (see Fig. 7).

Having identified the value $a_W = 16$ as the best suited for a finite lattice approximation, we computed the rescaling of the field, and found an anomalous dimension $\eta \in (0.25, 0.30)$. Although compatible with the exact result $\eta = 0.25$, our results favor values closer to $\eta = 0.30$. The first criterion used to address this issue, the eigenvalue being one, led to a window of acceptable anomalous dimension (0.25, 0.30) after a further assumption that there are 2 marginal directions. This further assumption comes as a particularity of the two-dimensional linear sigma model and should not show up in other models. The matching criterion 3(b), which turned out to be a very sensitive criterion (see Fig. 11), clearly favored $\eta \sim 0.30$.

After all this previous study, we present the final results for the critical exponents,

$$\eta \in (0.25, 0.30) \tag{21}$$

$$\nu = 1.00(2) \tag{22}$$

$$\lambda_2 = 1.0(4) \tag{23}$$

$$\lambda_3 = 1.0(4) \tag{24}$$

Table IV. FP Hamiltonian at $a_W = 16$[a]

Operator	K	Operator	K	Operator	K
1	0.16(12)	8	0.06(4)	24	−0.017(5)
2	0.99(8)	9	0.05(2)	25	−0.007(3)
3	−0.22(3)	11	0.07(4)	27	0.005(2)
4	0.03(5)	12	−0.06(2)	33	0.029(5)
5	−0.0016(3)	15	0.12(2)	37	−0.012(4)
6	−0.90(5)	16	0.03(1)		
7	−0.17(4)	21	0.03(1)		

[a] Only the non-vanishing couplings are displayed.

where the error merely indicates the uncertainty in the determination of the anomalous dimension, which in turn, depends on the statistical error and the lack of criticality, as explained. We would like to emphasize that all the rest of systematic errors have been considered and shown to be smaller (see the discussion at the end of the last section). we also computed the FP Hamiltonian. and found that it may be parametrized with a few operators (see Table IV). Finally, we provide arguments that within a Bell–Wilson RGT one can only compute a finite number of exponents, the rest are not accessible to numerical methods due to error e(4). Most likely, this number reduces the accessible eigenvalues to the ones we quote, although it is possible that this is just a reflection of the modest statistics used.

6.2. Perspective and Outlook

By optimizing the transformation used we have been able to get a great deal of information, including precise calculations for critical exponents, FPs, etc. with modest statistics, and more importantly, to have under control the different source of errors. There are, however, some problems that we should emphasize. Concerning the determination of the anomalous dimension, our results favor values of $\eta \sim 0.30$, although $\eta = 0.25$ is still acceptable. Higher statistics and a more accurate determination of the critical surface should resolve this issue. Another important point concerns real space renormalization group methods as they seem to present a limitation concerning the number of, generally irrelevant, critical exponents accessible within finite lattice approximations. Deeper understanding of the properties of RGTs are necessary with the ultimate goal of proposing RGTs with better convergence properties and good short-rangeness behaviour, as is discussed in the final appendix.

There are similar MCRG calculations for models of unconstrained spins using momentum RGTs.[16] As discussed, RGTs in momentum space have different properties and are not directly comparable. Closer works to compare ours with are MCRG calculation for 3d Ising models using real space RGTs[17, 18] and the most recent update.[19] Although the large statistics and big lattices reported in those papers are completely unattainable with our resources, at a more conceptual level there are interesting analogies we can draw. The RGT transformation used in those works is a majority rule, which is the spin-constrained version of the Bell–Wilson RGT at $a_W = \infty$. We have seen that this is a very unfavorable case concerning the short-ranged properties of the effective interactions and the approach to the FP, so it may be the case as well for the constrained model (which can be obtained as the $\lambda \to \infty$ case of the unconstrained one). Let us recall that this is not at odds with the good matching for expectation values of operators. We find a surprisingly accurate matching for 3 RGTS even at $a_W = \infty$, despite that other criteria shows that we do not reach a FP after 3RGTs. Our best value for the matching singles out an anomalous dimension slightly off from its exact value. Similarly, in 3d Ising MCRG calculations the anomalous dimension comes slightly off from its more accepted value.[20] Secondly, only two even parity eigenvalues may be computed, a result which seems in agreement with the difficulties mentioned concerning the convergence of higher irrelevant eigenvalues; It would be interesting to perform similar calculations using more elaborate RGTs.

Although, as discussed, some questions demand further clarification, we have shown that with a suitable knowledge of the RGT, finite lattice approximations provide a systematic expansion to perform calculations in the RG. We hope that this paper will help to arouse and inspire further work in this field, which will allow application of these methods to more general models.

APPENDIX A. THE STRONG COUPLING EXPANSION

We determine the CS by means of a high temperature expansion (HTE) of the susceptibility,

$$\chi = \sum_{i=0}^{\infty} \chi_1^{(i)} \kappa^i \tag{25}$$

where $\chi_1^{(i)}$ depend on λ through integrals like $I_n(\lambda) = \int_0^\infty d\phi\, \phi^n e^{-S[\phi]}$. Baker and Kincaid,[21] have tabulated its first 11 coefficients, and in such a case, only even integrals up to $n = 12$ have to be considered.

Had we computed the whole series, the critical coupling is obtained from the ratio method,[22]

$$\kappa_c(\lambda) = \lim_{n \to \infty} r_n, \qquad r_n \equiv \chi_1^{(n-1)}/\chi_1^{(n)} \tag{26}$$

but in our case must be extrapolated from finite n ratios. In such a case corrections to the preceeding formulae are correlated with the form of the closest singularity of the susceptibility to the origin in the complex κ plane. It is assumed that,

$$r_n = \kappa_c(\lambda)\left(1 + \frac{1-\gamma}{n} + \sum_j \frac{c_j}{n^j}\right) \tag{27}$$

plus some exponential corrections $\exp(-na)$ arising from singularities farther, provided that within the disk $|\kappa| = \kappa_c(\lambda)$ there are no further singularities. This is, unfortunately not the case for a *PSQ* (plane square) lattice (as it is always for loose-packed lattices), due to the presence of an antiferromagnetic singularity at $\kappa = -\kappa_c(\lambda)$, which brings in nonanalytical oscillating power law corrections in Eq. (27), of the type,

$$r_n \sim \frac{(-1)^n}{n^{\gamma+\Phi}} \tag{28}$$

Φ is the critical exponent associated to the antiferromagnetic singularity.

The ratios in Eq. (26). of the expansion in Eq. (25), are nearly constant with a monotonic decreasing oscillating trend. Using a double ratio method,[22] a rough estimate of the critical coupling may be obtained κ_{re}. We define then a new variable through,

$$z = \frac{2\kappa}{1 + (\kappa/\kappa_{re})} \tag{29}$$

so that we send the antiferromagnetic singularity almost to ∞, and thus the susceptibility expressed in this new variables eliminates the oscillating term in Eq. (28) as it picks up a large exponential correction.

We can extrapolate now by using Eq. (27) for $n \geqslant 5$ and we estimate the error from comparing extrapolations including different inverse powers in n. We also analyzed the ratio method if instead of κ_{re}, we input the new better estimate, but nothing is gained within error bars. In any case, Just to compare with known results, we obtained for $\lambda = \infty$ (Ising limit),

$$K_c = 0.4407(2) \tag{30}$$

in agreement with the exact result $K_c = 0.4406868$.

APPENDIX B. THE NON-CONVERGENCE OF EIGENOPERATORS

In this appendix we show in an explicit example how exact eigenoperators of the T-matrix may not converge. We explicitly show as an example the Gaussian Model, defined as the most general translational-invariant quadratic Hamiltonian

$$\mathscr{H} = \tfrac{1}{2} \sum_n \sum_r \rho(r)\, \phi(n)\, \phi(n+r) \tag{31}$$

where the sum is over sites of the corresponding lattice. Under k-iterations of a linear RGT the model transforms into itself,

$$\mathscr{H}_k = \tfrac{1}{2} \sum_n \sum_r \rho_k(r)\, \vartheta(n)\, \vartheta(n+r) \tag{32}$$

It is possible to derive an exact RG-equation for the RGT used in this paper,[4] which is not difficult to generalize to a completely general linear RGT.[6]

We can actually solve the equations and find the exact FP and eigenoperators. We just quote the final result for the j-eigenoperator[6]

$$\delta_j \rho(p) = \rho^*(p)^2\, g_j(p), \qquad g_j(p) = \sum_{l=-\infty}^{+\infty} \frac{1}{(p+2\pi l)^{(4-2j)}} \prod_{\mu=1}^{d} g(p_\mu + 2\pi l_\mu) \tag{33}$$

where the equation is expressed in momentum space, $j = 0, 1, \ldots$, the dimension of the system is d ($d=2$ in our case), and ρ^* is the FP value of the couplings which is not directly relevant for our problem and will appear elsewhere. The function $g(x)$ depends on the RGT. For the Bell–Wilson RGT Eq. (13) we have[4]

$$g(x) = \frac{\sin^2(x/2)}{(x/2)^2} \tag{34}$$

In this case, eigenoperators Eq. (33) are well defined for $j=0$ (relevant), $j=1$ (marginal), $j=2$ (irrelevant), but the sum in Eq. (33) fails to converge for $j>2$. Any numerical method will necessary fail to get this eigenoperator right, as it has just a formal meaning. This conforms very well to the numerical results reported in.[4]

To remedy this situation, one has to consider other RGTs, which have overlapping cells (see Fig. 18). Let us mention that these transformations

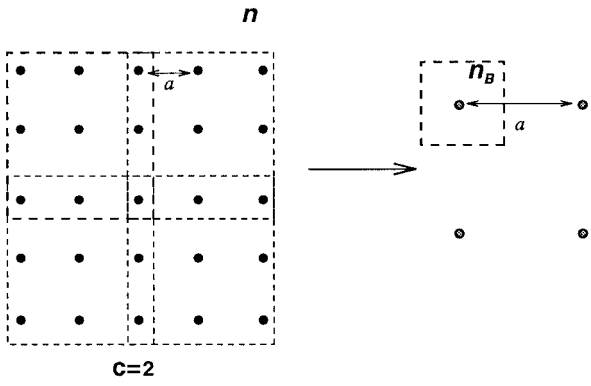

Fig. 18. The simplest case of overlapping RGT.

have appeared in the context of perfect actions.[5] For such a case one gets a g-function

$$g(x) = \frac{\sin^4(x)}{(x/2)^4} \tag{35}$$

so now, for example, from Eq. (33) the $j = 3$ eigenoperator does converge, opposite to what it happens with Bell–Wilson RGT. In other words, the eigenvalue with $j = 3$ becomes now accessible to numerical methods. In fact, the RGT in Fig. 18 is just the simplest case of an overlapping RGT. One may define more elaborated RGTs so that the g-function Eq. (34) becomes more convergent.[6]

Let us call that RGTs in momentum space are an extreme case of overlapping RGTs. In such a case, it is easy to prove that eigenoperators are perfectly convergent for any value of j. However, this is a very unfavorable case concerning the short-rangeness of the effective actions generated, because the decay ansatz Eq. (12) gets replaced by an algebraic decay. It seems then, that there is some kind of uncertainty principle concerning RGTs; One may have very well behaved RGTs concerning how short-ranged the effective interactions are at the expense of some eigenoperators having just a formal meaning, or one may choose RGTs having very well defined set of eigenoperators at the expense of having poor short-ranged behaviour of the Hamiltonian generated along the RG flow.

ACKNOWLEDGMENTS

We acknowledge M. Bowick for a careful reading of the manuscript. We also acknowledge interest and discussions with J. Comellas, D. Espriu,

P. Hasenfratz and R. Toral. The research of A.C., E.G. and A.T. was supported by the U.S. Department of Energy under Contract No. DE-FG02-85ER40237.

REFERENCES

1. K. G. Wilson and J. Kogut, *Phys. Rep.* **12**:75 (1974).
2. R. H. Swendsen, *Phys. Rev. Lett.* **42**:829 (1979).
3. A. Gonzalez-Arroyo and M. Okawa, *Phys. Rev. D* **35**:672 (1987).
4. T. L. Bell and K. G. Wilson, *Phys. Rev. B* **11**:3431 (1975).
5. P. Hasenfratz and F. Niedermayer, *Nucl. Phys. B* **414**:785 (1994).
6. A. Travesset, Ph.D. thesis, Universitat de Barcelona (1997), unpublished.
7. R. H. Swendsen, *Phys. Rev. Lett.* **52**:2321 (1984).
8. A. Hasenfratz *et al.*, *Phys. Lett. B* **140**:76 (1984).
9. H. Shenker and J. Tobochnik, *Phys. Rev. B* **22**:4462 (1980); J. Hirsch and H. Shenker, *Phys. Rev. B* **27**:1736 (1983).
10. F. Wegner, in *Phase Transitions and Critical Phenomena*, C. Domb and M. S. Green, eds. (1987), Vol. 6, p. 7.
11. A. Travesset, *Nucl. Phys. B* **63A-C** (Proc. Suppl.):640 (1998).
12. G. Murthy and R. Shankar, *Phys. Rev. B* **32**:5851 (1985).
13. A. Gocksch and U. M. Heller, *Nucl. Phys. B* **275**:219 (1986).
14. R. Brower and P. Tamayo, *Phys. Rev. Lett.* **62**:1087 (1989).
15. U. Wolff, *Phys. Rev. Lett.* **62**:361 (1989).
16. D. Espriu and A. Travesset, *Phys. Lett. B* **356**:329 (1995).
17. G. S. Pawley *et al.*, *Phys Rev. B* **29**:4030 (1984).
18. C. Baillie *et al.*, *Phys. Rev. B* **45**:10438 (1992).
19. R. Gupta and P. Tamayo, cond-mat 9601048.
20. R. Guidaa and J. Zinn-Justin, cond-mat 9803240.
21. Baker and J. M. Kincaid, *J. Stat. Phys.* **24**:469 (1981).
22. D. S. Gaunt and A. J. Guttmann, in *Phase Transitions and Critical Phenomena*, C. Domb and M. S. Green, eds. (1974), Vol. 3.